Liquation Cracking in Partial-Penetration Aluminum Welds: Effect of Penetration Oscillation and Backfilling

Surprisingly, the papillary- (nipple-) type penetration common in aluminum welds can oscillate along the weld and promote cracking that can be difficult to eliminate with filler metals

BY C. HUANG AND S. KOU

ABSTRACT. Aluminum alloys are susceptible to liquation cracking in the partially melted zone (PMZ), where grain boundary (GB) liquation occurs during welding. Liquation cracking near the weld root in partial-penetration aluminum welds was investigated. Gas metal arc welding (GMAW) with Ar shielding was conducted on binary Al-Cu Alloy 2219. Filler metals of various Cu and Si contents were used, including 1100, 2319, 4145, 4047, and 2319 plus extra Cu. The results were as follows. First, the papillary type penetration common in aluminum GMAW was observed and it oscillated up and down, resulting in a wavy weld root along the weld. Second, liquation cracking was observed in welds with penetration oscillation but not in welds without. Third, liquation cracking most often occurred in between waves of the wavy weld root. Fourth, changing the filler metal did not eliminate liquation cracking. Fifth, the PMZ grains near the weld root were deformed, suggesting that weld metal solidification induced localized tensile stress/strain in the liquated PMZ near the weld root. Sixth, a mechanism was proposed to explain the effect of penetration oscillation: the PMZ GBs near the weld root immediately behind the oscillating penetration front of the weld pool are both in tension and liquated, and cracking can occur if liquation is significant. Seventh, highly alloyed filler metals that delay weld metal solidification (4145, 4047, and 2319 plus extra Cu) resulted in large liquation cracks backfilled with much eutectic-rich material. Eighth, a mechanism was proposed to explain the large cracks: backfilling of cracks by an abundant solute-rich interdendritic liquid from the nearby weld metal can cause melting around the cracks and worsen GB liquation and, hence, liquation cracking, which in turn increases backfilling.

C. HUANG is a Graduate Student at, and S. KOU is a Professor and Chair of, the Department of Materials Science and Engineering, University of Wisconsin-Madison, Madison, Wis.

Introduction

The partially melted zone (PMZ) is the region immediately outside the fusion zone, where liquation occurs during welding because of heating above the eutectic temperature (or the solidus temperature if the workpiece is completely solutionized before welding) (Ref. 1). Liquation can occur along the grain boundary (GB) as well as in the grain interior. Grain boundary liquation can cause cracking in the PMZ. PMZ cracking has also been called edge-of-weld cracking (Ref. 2), base-metal cracking (Ref. 3), hot cracking (Ref. 4), heat-affected zone cracking (Ref. 5), and liquation cracking (Ref. 6). The name liquation cracking is used in the present study.

Aluminum alloys are known to be susceptible to liquation cracking in the PMZ during welding. Liquation cracking in aluminum welds has been a subject of great interest in welding (Refs. 1–16).

Huang and Kou (Refs. 16–20) recently studied PMZ liquation in the welds of Alloys 2219, 2024, 6061, and 7075, including the liquation mechanisms, GB solidification, GB segregation, and PMZ weakening caused by GB segregation. Alloy 2219 is used to investigate liquation cracking in the present study.

Metzger (Ref. 3) reported the effect of the weld metal composition on liquation cracking in aluminum welds. Liquation cracking occurred in full-penetration gas tungsten arc (GTA) welds of Alloy 6061 made with Al-Mg fillers at high dilution ratios but not with Al-Si fillers at any dilution ratios. Metzger's study has been confirmed by subsequent studies on 6061 and similar alloys such as 6063 and 6082 (Refs. 5, 7–12).

Gittos and Scott (Ref. 5) conducted the circular-patch test (Ref. 21) on an aluminum alloy close to Alloy 6082 in composition. Full-penetration GTA welds were made with filler metals of Al-5Mg and Al-5Si. As in the study of Metzger (Ref. 3), liquation cracking occurred in the welds made with the Al-5Mg filler at high dilution ratios (about 80%) but not in the welds made with the Al-5Si filler at any dilution ratios.

Katoh et al. (Ref. 7), Kerr et al. (Ref. 8), and Miyazaki et al. (Ref. 9) conducted the Varestraint test (Refs. 22, 23) on 6000-series alloys including Alloy 6061. Partial-penetration GTA and gas metal arc (GMA) welds were made. Longitudinal liquation cracking occurred with a 5356 filler but not with a 4043 filler.

The present study deals with liquation cracking near the weld root in partial-penetration aluminum welds, focusing on the effect of penetration oscillation and backfilling on liquation cracking. The simple binary Al-Cu Alloy 2219 was selected to help understand liquation cracking more easily. However, similar cracking has also been observed in multicomponent aluminum alloys and the results will be reported elsewhere. Liquation cracking in full-penetration aluminum welds will also be reported elsewhere (Ref. 24).

KEY WORDS

Aluminum Alloys
Gas Metal Arc Welding (GMAW)
Liquation Cracking
Papillary Penetration
Penetration Oscillation

Experimental Procedure

The workpiece was Alloy 2219-T851. "T8" stands for solution heat treating and cold working, followed by artificial aging, and "Tx51" stands for stress relieving by stretching (Ref. 25). The actual compositions of the alloys are listed in Table 1 along with those of the filler metals. The workpiece was 20 cm long (8 in.), 10 cm wide (4-in.), and 9.5 mm thick (⅜ in.). It was welded in the as-received condition.

Bead-on-plate GMAW was carried out perpendicular to the rolling direction of

the workpiece. Figure 1 shows that the workpiece was neither clamped down to any fixture nor subjected to any augmented strains such as bending. It simply rested on the top of two aluminum supports mounted on a carriage. A semiautomatic welding gun was mounted on a stationary support and the workpiece moved at a constant speed under the gun.

The welding parameters were 7.41-mm/s (17.5-in./min) travel speed, 30-V arc voltage, 250-A average current, and Ar shielding. The wire diameter was 1.2 mm (3/64 in.) and the feed rate was 18.6 cm/s (440 in./min). The contact tube to workpiece distance was about 12.7 mm (0.5 in.), and the torch was held perpendicular to the workpiece.

The filler metals were 1100, 2319, 4145, 4047, and 2319 plus extra Cu. Filler metal 1100 has essentially no Cu, and the matching filler 2319 has as much Cu as Alloy 2219. Filler metal 4145 has about 4 wt-% Cu and 10 wt-% Si, and filler metal 4047

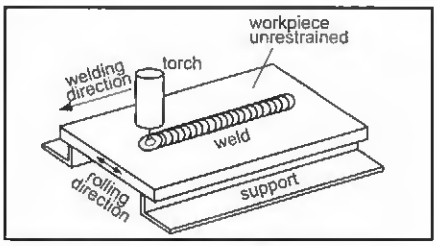

Fig. 1 — Welding with workpiece unrestrained to avoid interfering with interaction between the weld metal and partially melted zone during welding.

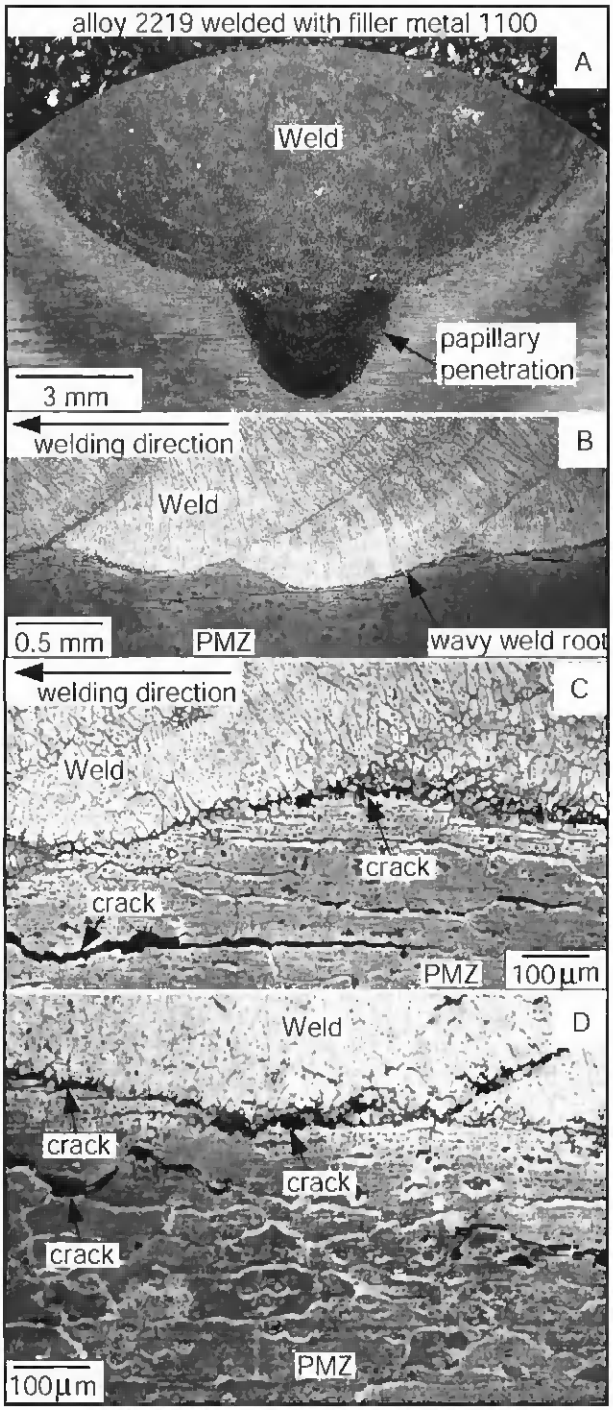

Fig. 2 — Weld made with filler metal 1100: A — transverse macrograph; B — longitudinal macrograph; C — longitudinal micrograph; D — transverse micrograph.

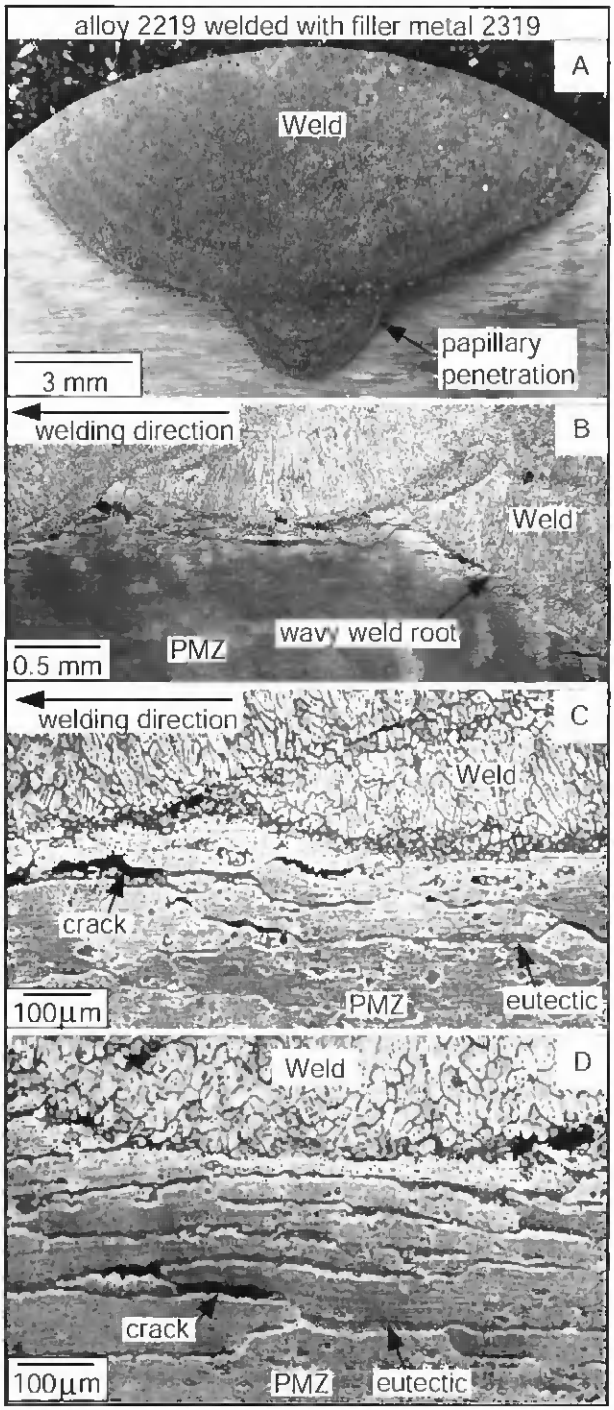

Fig. 3 — Weld made with filler metal 2319: A — transverse macrograph; B — longitudinal macrograph; C — longitudinal micrograph; D — transverse micrograph.

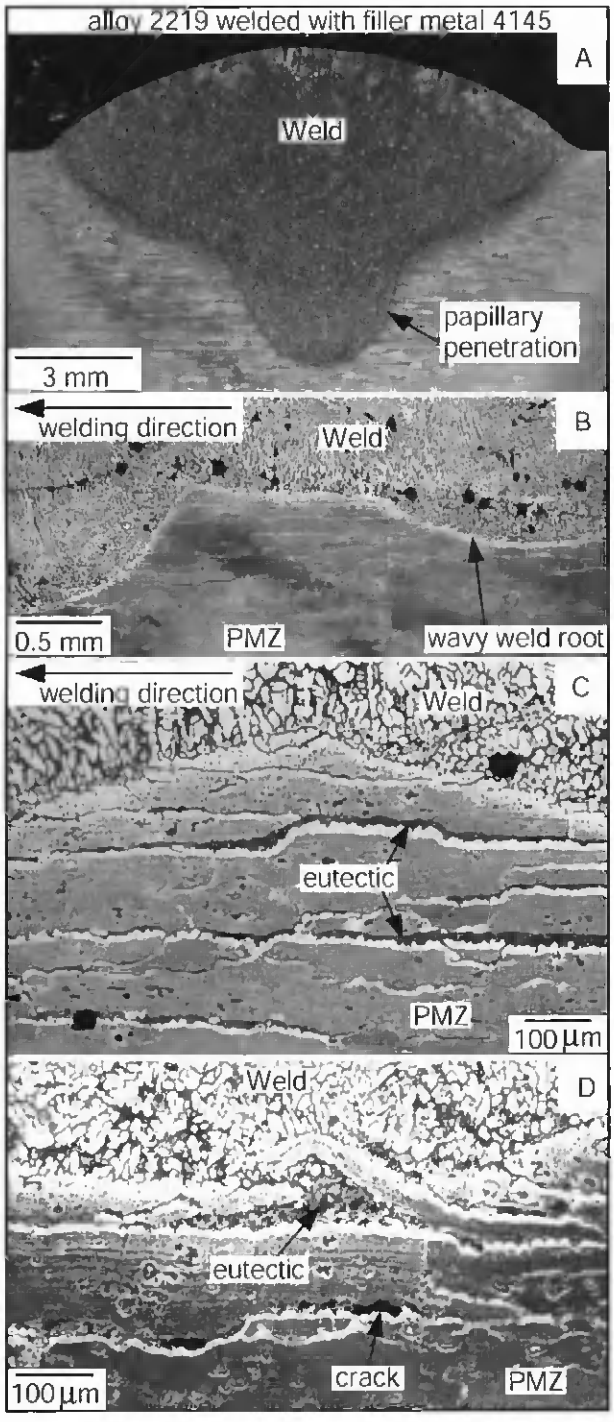

Fig. 4 — Weld made with filler metal 4145: A — transverse macrograph; B — longitudinal macrograph; C — longitudinal micrograph; D — transverse micrograph.

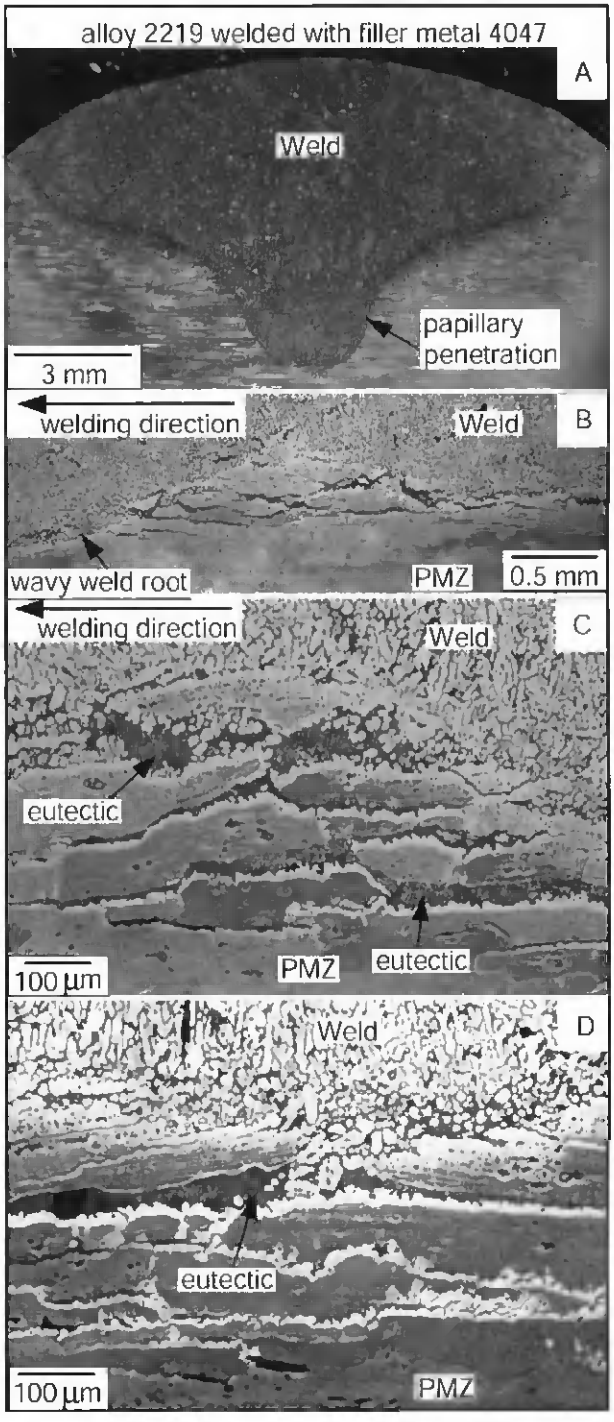

Fig. 5 — Weld made with filler metal 4047: A — transverse macrograph; B — longitudinal macrograph; C — longitudinal micrograph; D — transverse micrograph.

Table 1 — Chemical Compositions of the Workpiece and Welding Wire in Wt-%

	Si	Cu	Mn	Mg	Cr	Zn	Ti	Fe	Zr
Workpiece									
2219	0.09	6.49	0.32	0.01	–	0.03	0.06	0.14	0.13
Filler Metals									
1100	0.08	0.08	0.01	–	–	0.02	–	0.52	–
2319	0.10	6.30	0.30	–	–	–	0.15	0.15	0.18
4145	9.9	3.9	0.01	0.05	0.01	0.04	–	0.2	–
4047	11.6	0.03	–	0.02	–	–	–	0.2	–

has about 12 wt-% Si. The extra Cu was a pair of Cu wires of 99.999 wt-% purity and 1 mm diameter that were positioned in a 2-mm-wide by 1-mm-deep rectangular groove along the centerline of the workpiece surface. The Cu wires were gas tungsten arc welded (GTAW) three times to melt and mix with the surrounding base metal. The condition for GTAW was 14 V, 160 A, DC electrode negative, and 4.2-mm/s (10-in./min) travel speed with Ar

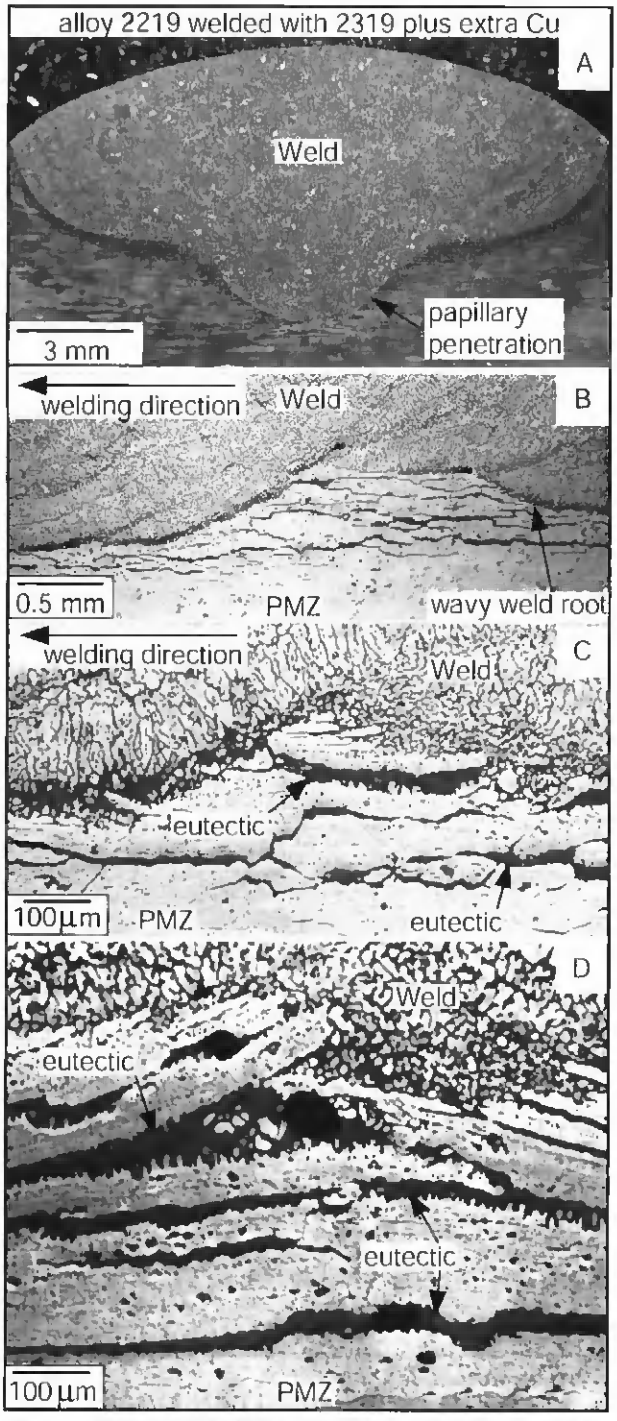

Fig. 6 — Weld made with filler metal 2219 plus extra Cu: A — transverse macrograph; B — longitudinal macrograph; C — longitudinal micrograph; D — transverse micrograph.

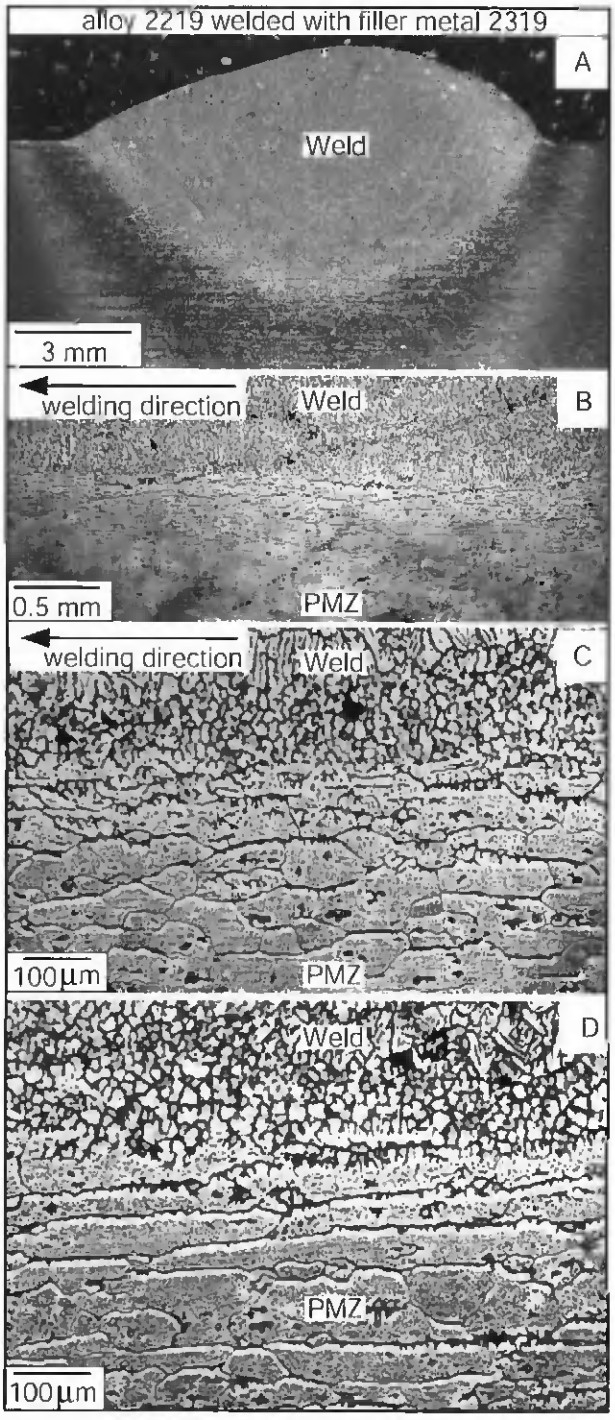

Fig. 7 — Smooth weld made with filler metal 2319 without papillary penetration and liquation cracking: A — transverse macrograph; B — longitudinal macrograph; C — longitudinal micrograph; D — transverse micrograph.

shielding. The resultant weld head was about 6 mm wide at the top and 4 mm deep, which was well within the GMA weld made subsequently with filler metal 2319 in order to include all the extra Cu into the GMA weld.

A workpiece 20 cm long (8 in.), 10 cm wide (4 in.), and 7.9 mm thick (⅝ in.) was also welded. The welding parameters were 7.20-mm/s (17-in./min) travel speed, 26.5-V arc voltage, 195-A average current, and Ar shielding. The welding wire was a 1.2-mm-diameter wire of Alloy 2319, and the wire feed rate was 13.5 cm/s (320 in./min). The contact tube to workpiece distance was 25.4 mm (1 in.), and the torch pointed forward at a 15-deg angle from the vertical line instead of vertically down.

The resultant welds were cut, polished, and etched with a solution of 0.5 vol-% HF in water for microstructural examination by optical microscopy. Transverse cross sections of the welds were taken with a digital camera.

The concentration of any element, E, in the weld metal was calculated as follows:

$$\%E \text{ in weld metal} = (\%E \text{ in base metal}) \times [A_b / (A_b + A_f)] + (\%E \text{ in filler metal}) \times [A_f / (A_b + A_f)] \quad (1)$$

where A_b and A_f are the areas in the weld

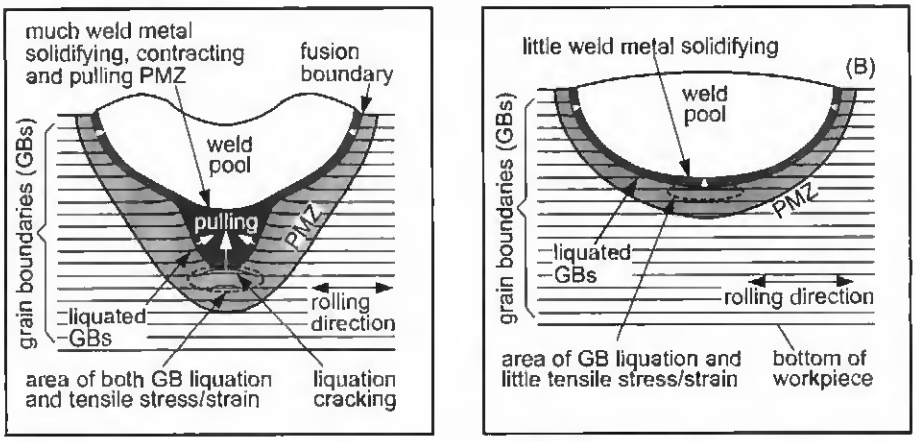

Fig. 8 — Localized stress/strain in the partially melted zone (PMZ) in the transverse cross section of a solidifying weld pool traveling perpendicular to the rolling direction. A — Papillary penetration; B — smooth weld bottom.

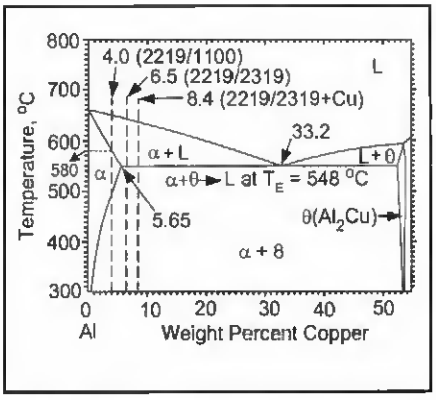

Fig. 9 — Aluminum-rich side of Al-Cu phase diagram (Ref. 38).

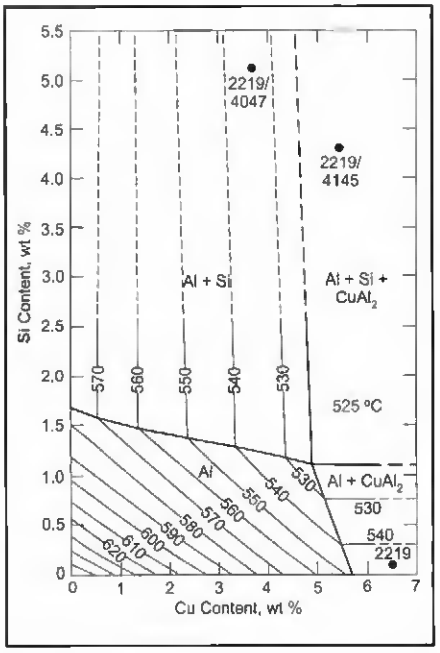

Fig. 10 — Al-Cu-Si solidus temperature map (Ref. 39). 2219/4145 and 2219/4047 denote welds of Alloy 2219 made with filler metals 4145 and 4047, respectively.

transverse cross section that represent contributions from the base metal and filler metal, respectively. The ratio $A_b/(A_b + A_f)$ is the dilution ratio. Areas A_b and A_f were determined from the transverse macrograph by using commercial computer software.

Results and Discussion

Characteristics of Weld Penetration

Figures 2 through 6 show the results of the bead-on-plate welds made in the 9.5-mm (⅜-in.) workpiece with various filler metals. The transverse macrographs of the welds in Figs. 2A through 6A show a papillary- (nipple-) type penetration. Some of the papillary penetrations were shallower than others. The depth appeared to vary to some extent with the filler metal, but no apparent patterns of variations were found.

The longitudinal macrographs of the same welds in Figs. 2B through 6B show that the weld root was wavy along the weld instead of smooth. This surprising result indicates that papillary penetration was not steady but oscillated up and down along the weld.

In GMAW, spray transfer is the most commonly used mode of metal transfer from the welding wire to the weld pool. In GMAW of aluminum alloys with Ar shielding, which is the most widely used process for welding aluminum alloys, the arc energy is concentrated along the core of the arc because of the relatively low thermal conductivity of Ar. Consequently, the Ar arc plasma has a very high-energy core and an outer mantle of lesser thermal energy. This helps to produce a stable, axial transfer of metal droplets through an Ar arc plasma. The resultant weld transverse cross section is often characterized by a papillary-type penetration pattern (Ref. 26).

While the papillary-type penetration pattern in GMAW of aluminum alloys is well-known, the oscillation of a papillary penetration along the weld is not (at least not to the best knowledge of the authors).

As shown in Figs. 2B through 6B, the penetration depth of the GMA welds made with Ar shielding oscillated rather than remaining constant. The causes for penetration oscillation can be fluctuations in, for instance, the welding current, welding wire melt rate, or droplet transfer. With the superheat and momentum of the filler metal droplets in spray transfer, these fluctuations can cause thermal and, hence, melting fluctuations at the pool bottom when the droplets penetrate the weld pool and impinge on the pool bottom. Fluctuations in the arc pressure can cause pool surface oscillation (Refs. 27–32), which may also affect heat transfer to the pool bottom.

Penetration Oscillation and Liquation Cracking

The longitudinal micrographs of the welds in Figs. 2C through 6C show liquation cracking in the PMZ near the weld root. The cracks were intergranular, ranging from open (Fig. 2C) to backfilled (Figs. 4C–6C). The transverse micrographs of the welds in Figs. 2D through 6D show similar characteristics of liquation cracking. It is evident from Fig. 2B and C through Fig. 6B and C that liquation cracking occurred most often in the area between waves of the wavy weld root.

Of all the filler metals used for welding Alloy 2219 in the present study, 2319 resulted in the least liquation cracking. It is known that many welds of Alloy 2219 fabricated with filler metal 2319 have been found crack-free. In the aerospace industry, such welds have been made by GTAW, which does not cause penetration oscillation. The authors have made such welds by full-penetration GMAW in circular-patch testing, and, of course, no penetration oscillation can occur in full-penetration welds. They have also made such welds by partial-penetration GMAW in which penetration oscillation was absent. What Fig. 3 shows clearly is that small liquation cracks can appear in partial-penetration GMAW of 2219 with 2319 and Ar if PMZ liquation is significant and penetration oscillation is clear (that is, the weld root shows clear waves along the welding direction).

The presence of liquation cracking in the full-penetration GTA welds of Metzger (Ref. 3) and Gittos and Scott

(Ref. 5), where neither the papillary penetration nor penetration oscillation exists, does not necessarily imply that the weld penetration type is not a dominant factor in liquation cracking. The present study by no means suggests liquation cracking cannot occur in aluminum welds unless the papillary penetration or penetration oscillation exists. As mentioned previously, liquation cracking has been observed in full-penetration aluminum welds by the authors and it will be reported elsewhere (Ref. 24).

Steady Penetration and Absence of Liquation Cracking

Figure 7 shows a bead-on-plate weld made in the 7.9-mm (5/16-in.) workpiece with filler metal 2319. As shown in the transverse macrograph in Fig. 7A, the bottom of the weld was smooth and without any papillary penetration. The use of the lower welding current (wire feed rate), the longer distance between the contact tube and the workpiece, and the 15-deg torch angle made the weld bottom smooth but reduced the penetration depth by about 40%.

As shown in the longitudinal macrograph in Fig. 7B, the weld root was smooth and without clear penetration oscillation along the weld. Neither the longitudinal micrograph of the weld in Fig. 7C nor the transverse micrograph in Fig. 7D shows any evidence of liquation cracking in the PMZ.

Another 2219 weld was made in the 9.5-mm-thick (3/8-in.) workpiece by gas-tungsten arc welding with Ar and filler metal 1100. The weld had a penetration depth about the same as that in the 2219 weld shown in Fig. 2. However, the weld was smooth — without a papillary penetration or a wavy weld root. No liquation cracking was observed. This will be discussed further elsewhere because of space limitations.

In summary, liquation cracking occurred in welds with a wavy weld root but did not occur in welds with a smooth weld root, and the effect of weld penetration oscillation on liquation cracking was thus demonstrated.

Deformation, Cracking, and Localized Stress/Strain in PMZ

According to Borland (Ref. 33), there are essentially three hot cracking theories — the shrinkage-brittleness theory, the strain theory, and the generalized theory that includes the relevant ideas from the first two theories. According to the generalized theory, cracking can take place in a material in which continuous liquid films separate grains or in which some solid-solid bridges exist between grains (Ref. 33). When the localized tensile stress/strain in the material exceeds its resistance to cracking, hot cracking occurs.

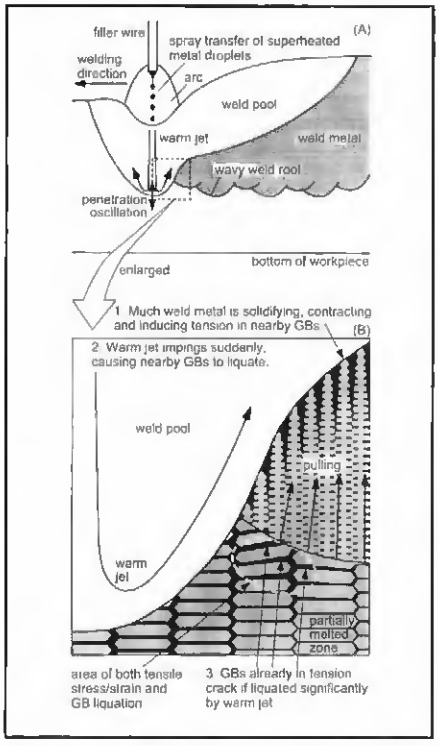

Fig. 11 — Mechanism of liquation cracking near weld root induced by penetration oscillation and grain-boundary liquation. A — Overview; B — enlarged view (with cracks backfilled).

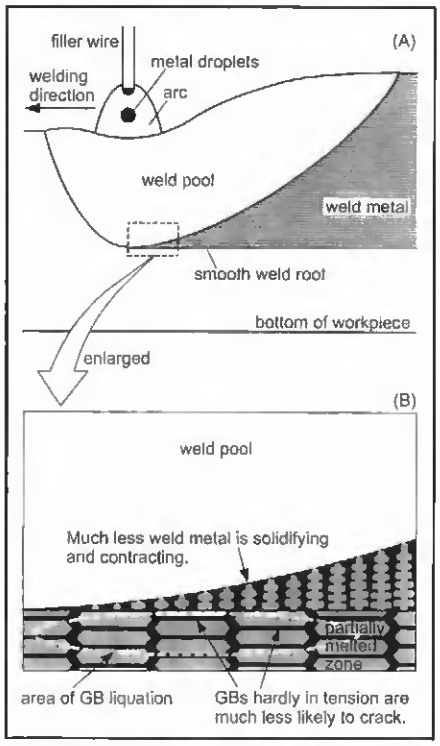

Fig. 12 — Liquation cracking is much less likely to occur without penetration oscillation. A — Overview; B — enlarged view.

Since the workpiece was not bent during welding to cause cracking as in Varestaint testing, the PMZ microstructure and cracks were not changed by any external forces and thus can provide qualitative information about the localized stress/strain in the PMZ that caused liquation cracking. The use of a freestanding workpiece does not eliminate the self-induced stress/strain during welding. However, liquation cracking occurs in an area in the PMZ near to the weld root, about 500 μm based on Figs. 2 through 6. It is likely that in the PMZ *near to the weld root*, the contraction of the solidifying weld metal dominates the tensile stress/strain during welding. This is because the solidification shrinkage and thermal contraction of aluminum alloys are both high and because no external stress/strain was applied during welding. The solidification shrinkage of aluminum is as high as 6.6% (Ref. 34). The thermal expansion coefficient of aluminum is roughly twice that of iron base alloys.

Before preceding any further, it should be pointed out that analysis of the localized stress/strain in the PMZ of a weld with penetration oscillation is beyond the scope of the present study. As already shown, liquation cracking occurred in welds with clear penetration oscillation but did not occur in smooth welds. The authors are unaware of any liquation cracking theories that consider the localized stress/strain in welds with penetration oscillation. They are also unaware of any methods for calculating or measuring the localized stress/strain in welds with penetration oscillation. The thermomechanical properties of semisolids such as the liquated PMZ and the solidifying weld metal are unavailable in the first place. Figures 2 through 6 show that liquation cracking occurred most often in the tiny area between waves along the wavy weld root, which can be far too small, too hot, and inaccessible for stress/strain measurements. Therefore, liquation cracking will be discussed based on the localized stress/strain in the PMZ near the weld root that was deduced from the deformed grains and cracks. In the study of Gittos and Scott (Ref. 5), the phrase "tensile strains arising from weld metal solidification" was used to qualitatively describe the localized stress/strain in the PMZ.

Figures 3D through 6D showed that the PMZ grains near the weld root were deformed; that is, pulled upward toward the tip of the papillary penetration. The deformed grains and the liquation cracks together suggest that weld metal solidification in the papillary penetration induced an upward tensile stress/strain in the PMZ near the tip of weld-pool penetration during welding and caused liquation cracking.

The localized tensile stress/strain in-

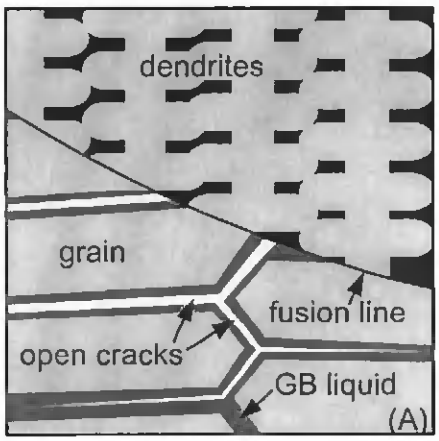

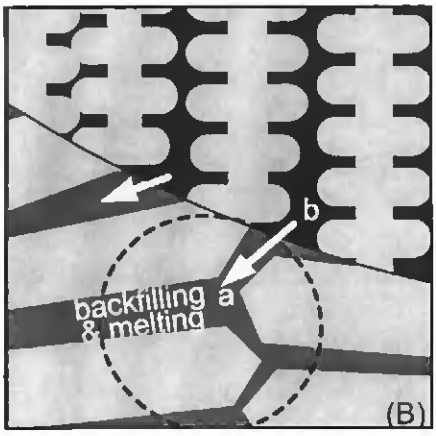

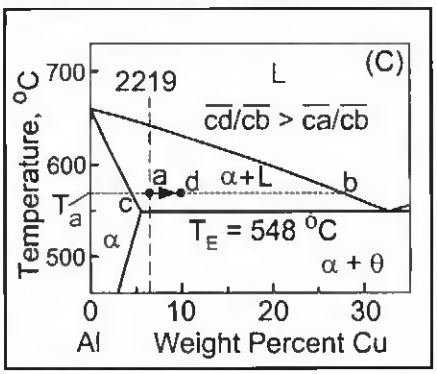

Fig. 13 — Backfilling of liquation cracks. A — No backfilling; B — backfilling and backfilling-induced melting; C — backfilling-induced increase in local average composition and increase in liquid fraction (melting) around cracks.

duced in the PMZ near the weld root increases with increasing extent of weld metal solidification. That is, the more solid that forms in the weld metal, the greater the localized tensile stress/strain is induced in the PMZ near the weld root by weld metal contraction. Meanwhile, the material resistance of the PMZ to cracking decreases with increasing extent of GB liquation. Thus, in the PMZ near the weld root the localized tensile stress/strain competes with the material resistance to cracking. If, near the weld root, much weld metal is already solidifying while the PMZ is still liquated

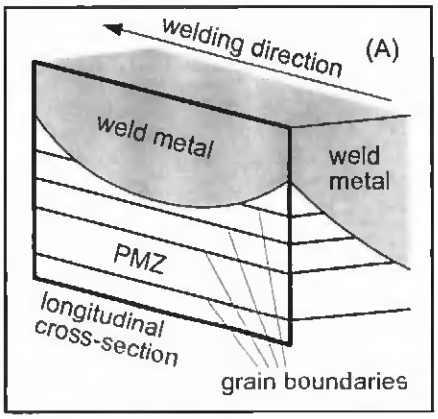

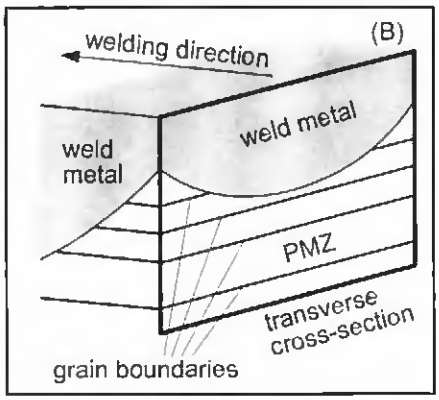

Fig. 14 — Access of grain boundaries in partially melted zone (PMZ) to weld metal. A — Longitudinal cross section; B — transverse cross section.

significantly, it is likely that the localized tensile stress/strain exceeds the material resistance to cracking and liquation cracking occurs. On the other hand, if little weld metal is solidifying while the PMZ is still liquated significantly, liquation cracking is unlikely to occur.

Figure 8 shows the transverse cross section of a solidifying weld pool traveling perpendicular to the rolling direction and the localized stress/strain in the PMZ near the weld root. As shown in Fig. 8A, the solidifying weld metal is significantly thicker inside the papillary penetration than elsewhere. (It is thicker because the weld metal in the papillary penetration, surrounded by a cooler PMZ on all sides as well as at the bottom, solidified rapidly. This is evident because the dendrite arm spacing was much finer inside the papillary penetration than near the bulk weld, but this will be shown elsewhere due to space limitations.) Because the solidifying weld metal is relatively thick inside the papillary penetration, it is already developing strength and contracting. The PMZ, however, does not contract as much as the weld metal does because solidification shrinkage is much less in the PMZ, in view of the much smaller volume of the GB liquid than the weld pool. Consequently, tensile stress/strain is induced in the PMZ near the weld root. This tensile stress/strain can be harmful because it is concentrated near the tip and normal to liquated GBs and thus can easily open them up.

On the other hand, as shown in Fig. 8B, the solidifying weld metal near the bottom of a smooth weld pool is much thinner, and thus it induces little tensile stress/strain in the PMZ nearby. This smooth weld without a papillary penetration is similar to that shown in Fig. 7. As shown in Figs. 7C and D, there was no liquation cracking in the weld. Very small waves and slightly deformed grains were observed occasionally along the weld, but no cracks were found.

As can be seen from Fig. 8A, liquation cracking is more likely to occur at the bottom of the fusion boundary than at the top. This was confirmed by the absence of liquation cracking at the top (micrographs not shown because of space limitations). Here, the direction of the tensile stress/strain is nearly parallel to the GBs, and the solidifying weld metal is thin. Furthermore, there is less liquation because of the steeper temperature gradients (that is, narrower PMZ) at the top (Refs. 1, 19).

Before leaving this section, it is worth discussing the weld made with filler metal 2319 plus extra Cu (Fig. 6) a little further. Making a solute-rich preweld before welding is an established technique for achieving the desired weld metal composition (Refs. 35–37). The severe liquation cracking (Fig. 6D) was not likely to be caused by the early formation of high-temperature, Cu-rich intermetallic compounds because the microstructure showed no evidence of such compounds in the weld metal. The liquation cracking was not likely to be caused by the residual stresses induced by the additional GTA passes, either. This is because the welds made with filler metals 4145 (Fig. 4D) and 4047 (Fig. 5D) also showed much liquation cracking — without making a solute-rich preweld before GMAW.

Solidus Temperatures and Liquation Cracking

According to Gittos and Scott (Ref. 5), the solidus temperature of the weld metal vs. that of the base metal has a strong effect on liquation cracking. Figure 9 shows the binary Al-Cu phase diagram (Ref. 38), which can be used to determine the solidus temperature of the weld metal in welds made with filler metals 1100, 2319, and 2319 with extra Cu. Likewise, Fig. 10 shows the solidus temperatures of Al-Cu-Si ternary alloys (Ref. 39), which can be used for the welds made with filler metals 4145 and 4047. The solid lines represent experimental data and the broken lines

are extrapolated from the solid lines.

Consider first the welds made in Alloy 2219 (Al-6.49Cu) with filler metal 1100 (Al-0.08Cu), 2319 (Al-6.30Cu), or 2319 with extra Cu. With 1100, the weld metal composition was Al-4.0Cu (dilution ratio 60.6%). From Fig. 9, the solidus temperature of the weld metal is 580°C. Similarly, with 2319 the weld metal composition was Al-6.4Cu (dilution ratio 60.6%). Since the eutectic temperature 548°C is the lowest possible temperature for an equilibrium liquid phase to exist in this weld metal, it is taken as its solidus temperature for the purpose of discussion. With 2319 plus extra Cu, the weld metal composition was Al-8.4Cu (dilution ratio 56.8%). The solidus temperature of the weld metal is again taken as the eutectic temperature 548°C.

Consider now the welds made in Alloy 2219 (Al-6.49Cu-0.09Si) with filler metals 4145 (Al-3.9Cu-9.9Si) and 4047 (Al-11.6Si-0.03Cu). With filler metal 4145, the weld metal composition was Al-5.38Cu-4.31Si (dilution ratio 57.0%). As shown in Fig. 10, the solidus temperature of the weld metal was 525°C. Similarly, with filler metal 4047, the weld metal composition was Al-3.67Cu-5.11Si (dilution ratio 56.4%) and the solidus temperature was 534°C.

In order to double-check the accuracy of the extrapolated solidus temperatures in Fig. 10, the computer program *Pandat* (Ref. 40) was used. The program calculates phase diagrams and solidification paths based on thermodynamic models and data. The calculated solidus temperatures based on equilibrium solidification was 524°C for the weld made with filler metal 4145 and 534°C for the weld made with filler metal 4047, which confirmed the solidus temperatures in Fig. 10.

Gittos and Scott (Ref. 5) stated, "The proposed mechanism of HAZ cracking is that, during welding, grain boundary melting occurs in the HAZ and with certain base metal and weld metal compositions, it is possible for the base metal solidus to be below the weld metal solidus. Thus, when tensile strains arising from weld metal solidification are imposed on the HAZ, cracking occurs at such boundaries." In the weld made with filler metal 1100 in the present study, liquation cracking occurred and the weld metal did have a higher solidus temperature (580°C) than the base metal (548°C). In the welds made with filler metals 2319 and 2319 plus extra Cu, however, liquation cracking occurred but the weld metal did not have a higher solidus temperature than the base metal. In the welds made with filler metal 4145 and 4047, liquation cracking also occurred, but the weld metal did not have a higher solidus temperature than the base metal, either.

In fact, Miyazaki et al. (Ref. 9) have also stated: "When the A6061 alloy was actually GMA welded using 5356 filler metal, longitudinal cracking was observed, but, contrary to Gittos et al., it was not observed that the solidus temperature of the weld metal became higher than that of the base metal." It was suggested that constitutional liquation induced by low-temperature eutectic reactions in the base metal could have made the effective solidus temperatures of the base metals lower than those of the weld metal. While this is likely to be true for Alloy 6061, liquation occurs in Alloy 2219 at the eutectic temperature 548°C and is thus not lower than that of the weld metal.

It is worth pointing out that the solidus temperature is relevant for equilibrium solidification. However, equilibrium solidification is not likely to occur in welding in view of the high cooling rates during welding, and the terminal solidification occurs through eutectic reactions at temperatures well below the solidus temperature. The solidus temperatures of the weld metal and the base metal are discussed in this section only for the purpose of comparing the experimental results in the present study with the theory of Gittos and Scott (Ref. 5).

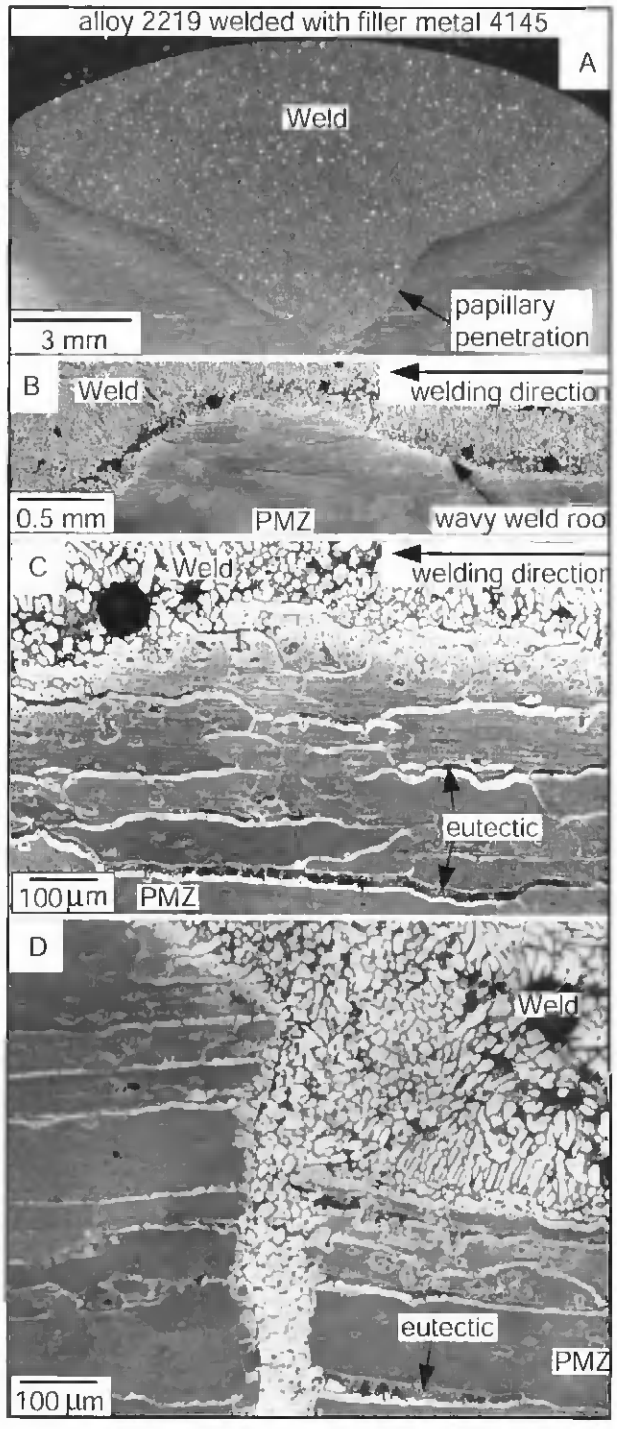

Fig. 15 — Weld in a butt joint made with filler metal 4145: A — transverse macrograph; B — longitudinal macrograph; C — longitudinal micrograph; D — transverse micrograph.

Effect of Penetration Oscillation on Liquation Cracking

A liquation-cracking mechanism is proposed in Fig. 11 to help explain the effect of penetration oscillation on liquation cracking. The emphasis is to explain the effect of penetration oscillation on liquation cracking observed in the present study — not to indicate that the conventional liquation cracking is generally incorrect.

As shown in Fig. 11A, in GMAW with spray transfer, weld-pool penetration can oscillate and result in a wavy weld root along the weld. A depression is formed at the pool bottom when the jet carrying the superheat of the liquid droplets impinges on the pool bottom. The area inside the rectangle is enlarged in Fig. 11B. As shown, much weld metal has already been solidifying, developing strength, contracting, and pulling the PMZ underneath. As such, significant tensile stress/strain is induced in the PMZ by weld metal solidification. When the warm jet impinges sud-

denly, the nearby GBs liquate upon heating by the jet. The PMZ GBs near the weld root immediately behind the oscillating weld-pool penetration front, as indicated in the figure, are subjected to both GB liquation and tensile stress/strain. If liquation is significant, the GBs can be severely weakened. Consequently, the localized tensile stress/strain can exceed the material resistance to cracking, and liquation cracking can occur. The incipient liquation cracks are likely to be small but they can gradually grow in size as weld metal solidification continues during welding. Figure 8A, in fact, is a transverse cross section showing the localized stress/strain in the PMZ near the weld root immediately behind the weld-pool penetration front.

Significant GB liquation is required for liquation cracking to occur even in the presence of clear penetration oscillation. For an aluminum alloy that can liquate significantly during welding, such as Alloy 2219, liquation cracking can occur easily in a weld with clear penetration oscillation. However, for an alloy that liquates much less significantly, liquation cracking may not occur even with clear penetration oscillation. This is because GBs are still well bridged together because of the relatively light GB liquation; that is, the PMZ resistance to cracking exceeds the localized tensile stress/strain. For instance, Alloy 6061 welded under the same condition as Alloy 2219 showed clear penetration oscillation. However, it neither liquated significantly nor exhibited liquation cracking. The results of Alloy 6061 will be reported elsewhere because of space limitations.

The absence of liquation cracking in a weld with a smooth weld root (Fig. 7) can be explained with the help of Fig. 12A, which shows a steady weld pool and the smooth weld root behind it. There is neither penetration oscillation nor a wavy weld root. The area inside the rectangle is enlarged in Fig. 12B. As compared to the case in Fig. 11B, there is much less weld metal solidification to induce tensile stress/strain in the PMZ and cause it to exceed the PMZ resistance to cracking. Farther down the weld, weld metal solidification increases but PMZ solidification also increases, and the PMZ tensile stress/strain still may not exceed the PMZ resistance to cracking.

As mentioned previously, liquation cracking most often occurred in the PMZ in the area between neighboring waves of the wavy weld root — Figs. 2B and C through Figs. 6B and C. During welding, this area corresponds to that near the weld root immediately behind the oscillating penetration front of the weld pool, which is essentially the area of both GB liquation and tensile stress/strain shown in Fig. 11B. Since the weld-pool penetration front subsequently solidifies as the next wave in the wavy weld root, this area ends up being between two neighboring waves. This explains why liquation cracking most often occurs in the area between neighboring waves of the wavy weld root.

In view of Fig. 11 and the rapid solidification of the weld metal near the weld root, it is likely there can still be enough weld metal solidifying before the warm jet impinges even when weld metal solidification is delayed by using a highly-alloyed filled metal. Thus, near the weld root the localized stress/strain induced in the PMZ by weld metal solidification, though reduced, can still exceed the PMZ resistance to cracking. This is consistent with the liquation cracking in the welds made with filler metal 4145, 4047, or 2319 plus Cu — Figs. 4–6. In fact, not only cracking occurred; the cracks were large and backfilled with much eutectic-rich material. This will be explained subsequently in the section below, headed "Backfilling-Induced Melting and Its Effect on Liquation Cracking."

Backfilling of Cracks

When liquation cracks are formed, a vacuum is created within them. A liquid connected to the cracks may or may not be sucked into them, depending on factors such as the quantity, viscosity, surface tension, and freezing temperature range of the liquid. Consequently, the cracks may remain open, as shown in Fig. 13A, or be backfilled as shown in Fig. 13B (and Fig. 11B as well).

If liquation cracks are backfilled, the liquid sucked into the cracks is most likely the solute-rich or even eutectic interdendritic liquid in the solidifying weld metal that is connected to the cracks rather than the liquid in the weld pool. This is because the material in the backfilled cracks was rich in eutectic — Figs. 3–6.

The higher the fraction of the solute-rich or eutectic interdendritic liquid in the solidifying weld metal at fusion boundary, the more backfilling can occur. Consider the welds made with filler metals 1100, 2319, and 2319 plus extra Cu. From the Al-Cu phase diagram shown in Fig. 9, the equilibrium partition ratio k = 5.65%/33.2% = 0.17 and the eutectic composition C_E = 33.2% Cu. For ease of discussion, the fraction of the liquid eutectic f_E will be used here as an indication of the amount of a solute-rich as well as a eutectic interdendritic liquid in the weld metal at the fusion line. The fraction of the liquid eutectic f_E can be calculated using the following form of the Scheil equation as an approximation (Ref. 1).

$$f_E = \left(\frac{C_o}{C_E}\right)^{\frac{1}{1-k}} \qquad (2)$$

According to Equation 2, for the weld metal of the weld made with filler metal 1100, C_o = 4.0% Cu and f_E = 0.08. For that with filler metal 2319, C_o = 6.4% Cu and f_E = 0.14, and for that with 2319 plus Cu, C_o = 8.4% Cu and f_E = 0.19. This suggests that backfilling should increase as the filler metal is changed from 1100 to 2319, and 2319 plus Cu. Figures 2, 3, and 6 do show this trend. However, the cracks were much larger and were backfilled with much more eutectic-rich material in the case of 2319 plus Cu than in the case of 2319. These differences, which cannot be explained based on the fraction of eutectic alone, will be explained later in the next section.

Savage and Dickinson (Ref. 35) suggested that the viscosity of the weld metal may also affect backfilling. Si decreases the viscosity of aluminum (Ref. 41) and it has been used to improve the fluidity of molten aluminum in metal casting. Since filler metal 4047 contained about 12% Si, it may increase the Si content of the interdendritic eutectic in the solidifying weld metal and thus help backfilling. Cu, on the other hand, increases the viscosity of aluminum (Ref. 41). This implies that filler metal 1100 should help backfilling while 2319 plus Cu should discourage it. However, liquation cracks were open with filler metal 1100 but backfilled with 2319 plus Cu. Therefore, the effect of Cu on viscosity seemed minor. Neither Si nor Cu has a significant effect on the surface tension of aluminum (Ref. 41).

Although some GBs may appear to be separated from the weld metal, they can, in fact, be connected to the solidifying weld metal during welding to allow backfilling. Figure 14A shows how GBs in a longitudinal cross section (Figs. 3C–6C) can have access to the weld metal. This makes sense only if the longitudinal cross section is not along the weld central plane. However, it is unlikely that a weld was cut precisely along the weld central plane. Furthermore, even if this were true, the penetration tip of the weld pool still did not necessarily move along the weld central plane. Rather, it could oscillate left and right as well as up and down as it traveled along the welding direction, in view of the unsteady nature of filler metal transfer during welding.

Similarly, Fig. 14B shows how GBs in a transverse cross section (Figs. 3D–6D) can have access to the weld metal. It makes sense only if the transverse cross section is not cut precisely at the bottom of a wave of the wavy weld root, but it is not very likely that this actually happened.

Backfilling-Induced Melting and Its Effect on Liquation Cracking

As mentioned previously, liquation cracks were much larger and backfilled

with much more eutectic-rich material when using highly alloyed filler metals 4145, 4047, and 2319 plus Cu — Figs. 4–6. This phenomenon will be explained with the help of the macrosegregation theory in metal casting. In metal casting, the flow of the solute-rich interdendritic liquid in the mushy zone (solid + liquid) can change the local average composition and liquid fraction in the mushy zone and cause eutectic-rich channels (freckles) to form in the ingots (Ref. 34).

Consider the backfilling illustrated in Fig. 13B. Point **a** is in the PMZ near the fusion boundary, where the temperature is T_a, and point **b** is in the solidifying weld metal nearby. Because of the high thermal conductivity of aluminum, the temperature at point **b** should be nearly identical to T_a. The white arrow from point **b** to point **a** indicates backfilling in the same direction. For simplicity, the composition fluctuation in the workpiece is neglected. Also, as in the derivation of the Scheil equation, the interdendritic liquid is assumed to be in equilibrium with the solid and to be locally homogeneous. In the Al-Cu phase diagram shown in Fig. 13C, point **a** indicates the local average composition of the area surrounding point **a** in Fig. 13B (indicated by the circle); that is, the workpiece composition (6.49% Cu). Likewise, point **b** in Fig. 13C indicates the composition of the interdendritic liquid at point **b** in Fig. 13B. As shown, the solute content at point **b** is much higher than the local average solute content at point **a**.

Consider first the hypothetical case in which the solute content of the interdendritic liquid at point **b** is identical to that of the local average solute content at point **a**. The local average liquid fraction at point **a** may increase momentarily when the interdendritic liquid at point **b** backfills the crack at point **a** but will quickly go back to its initial value before backfilling because there is only one local average liquid fraction at point **a** at a given temperature and composition. This can be seen from the following Scheil equation (Ref. 1):

$$f_L = \left(\frac{(-m_L)C_o}{T_m - T}\right)^{\frac{1}{1-k}} \quad (3)$$

where f_L is the liquid fraction, m_L (<0) the slope of the liquidus line in the phase diagram, C_o the solute content, T_m the melting point of pure aluminum, T temperature, and k the equilibrium partition ratio. According to Equation 3, at a given T and C_o, there is only one f_L.

However, as shown in Fig. 13C, the solute content of the interdendritic liquid at point **b** is much higher than the local average solute content at point **a**. Therefore, when the solute-rich interdendritic liquid flows from point **b** to point **a**, the local average solute content at point **a** can increase significantly, as represented by the arrow pointing from point **a** to point **d** in Fig. 13C. Using the simple lever-arm rule and the phase diagram as a rough indication, it can be seen that the fraction of liquid increases from **ca/cb** before backfilling to **cd/cb** after. Likewise, according to Equation 3, at a given temperature T, the local average liquid fraction f_L increases with increasing local average solute content C_o. As such, when the solute-rich interdendritic liquid flows from point **b** to point **a**, the local average liquid fraction at point **a** can increase significantly.

Therefore, when the solute-rich interdendritic liquid backfills a liquation crack, it can melt the material along the crack and cause more GB liquation. Since the GBs around the crack are in tension (Fig. 11B), further GB liquation causes further liquation cracking. Further liquation cracking, in turn, causes further backfilling — as long as there is sufficient solute-rich interdendritic liquid at the fusion boundary available for backfilling. This cycle can continue until the local fusion boundary cools down to the eutectic temperature and solidifies completely. This is especially true for welds made with a highly alloyed filler metal such as 2319 plus Cu (and 4145 and 4047), in which there is abundant solute-rich interdendritic liquid available at the fusion boundary for backfilling. This may explain the formation of large liquation cracks and their backfilling with much eutectic-rich material in Fig. 6 (and Figs. 4 and 5).

Weld in a Butt Joint with Papillary Penetration

In Fig. 8 the grains are continuous and pointing in the rolling direction, but in the case of a butt joint, the grains are discontinuous at the joint. It is thus interesting to see the effect of this discontinuity.

Figure 15 shows a weld in a butt joint made in the 9.5-mm (⅜-in.) workpiece with filler metal 4145. As shown by the transverse macrograph of the weld in Fig. 15A, the weld had a papillary penetration similar to those in Figs. 2A through 6A. As shown by the longitudinal macrograph in Fig. 15B, the weld had a wavy weld root similar to those in Figs. 2B through 6B.

The longitudinal micrograph in Fig. 15C shows that the weld had liquation cracks. The cracks were intergranular and mostly backfilled, similar to those in Fig. 4C. The transverse micrograph in Fig. 15D shows the weld bottom near the butt joint, the fusion boundary being higher on the left and lower on the right. Some weld metal leaked into the gap at the joint during welding. Liquation cracking was evident in the PMZ near the joint. The grains in the PMZ near the weld root were deformed, similar to those shown in Fig. 4D. Therefore, the characteristics of papillary penetration and liquation cracking in a weld in a butt joint are similar to those in a bead-on-plate weld. For a weld in a butt joint with a much larger joint gap, however, liquation cracking at the weld root may not occur.

The results in the present study also have practical implications for dual-pass welding in butt joints. In such welding the first pass is made from one side of the workpiece and the second pass from the opposite side. First, if the penetration tips from the two sides fail to overlap with each other, numerous liquation cracks can be present along the weld. Second, with sufficient overlapping between the two passes, the weld root of the second pass can still be wavy and thus can cause liquation cracking inside the first pass if GB liquation is significant near the weld root.

Conclusions

In view of the susceptibility of aluminum alloys to liquation cracking and the wide use of Ar-shielded GMAW for aluminum welding, liquation cracking was studied in partial-penetration aluminum welds made using GMAW with Ar shielding. Alloy 2219, which is a simple binary Al-Cu alloy easy to understand, was welded with filler metals of various Cu and Si contents, including 1100, 2319, 4145, 4047, and 2319 plus extra Cu. Liquation cracking near the weld root was examined in the transverse and longitudinal macrographs and micrographs of the resultant welds. The conclusions are as follows:

- The papillary-type penetration common in GMAW tends to oscillate up and down during welding. The penetration oscillation results in a wavy weld root along the weld.
- The combination of clear penetration oscillation and significant GB liquation promotes liquation cracking. Liquation cracking near the weld root has a much greater tendency to occur in welds with penetration oscillation than in welds without it.
- In welds with penetration oscillation, liquation cracking occurs most often in the PMZ between neighboring waves of the wavy weld root.
- In welds with penetration oscillation, adjusting the weld metal composition with the filler metal can be ineffective in eliminating liquation cracking, though it has been shown effective in full-penetration aluminum welds and perhaps in partial-penetration aluminum welds without penetration oscillation as well.
- In welds with papillary penetration, the deformation of the PMZ grains near

the weld root suggests that weld metal solidification induces tensile stress/strain in the PMZ near the weld root. The high solidification shrinkage and thermal contraction of aluminum alloys cause the solidifying weld metal to contract and pull the PMZ.

- Susceptibility to liquation cracking can vary significantly within the PMZ. Liquation cracking can be much more significant near the weld root than at the weld top, where there are less liquation and tensile stress/strain.
- In welds with penetration oscillation, liquation cracking can still occur even when the weld-metal solidus temperature is not higher than the base-metal solidus temperature, contrary to the full-penetration welds in the study of Gittos and Scott (Ref. 5).
- A liquation-cracking mechanism has been proposed to explain the effect of penetration oscillation on liquation cracking: the PMZ GBs near the weld root immediately behind the oscillating penetration front of the weld pool are subjected to both GB liquation and tensile stress/strain, and liquation cracking can occur if liquation is significant enough to weaken the GBs severely.
- When attempting to use highly alloyed filler metals to delay weld metal solidification and thus eliminate liquation cracking, large liquation cracks can form and be backfilled with much eutectic-rich material if penetration oscillation is present.
- A backfilling-induced melting mechanism has been proposed to explain the large backfilled cracks. Backfilling of liquation cracks by an abundant solute-rich interdendritic liquid from the nearby solidifying weld metal can cause melting along the cracks to worsen GB liquation and, hence, liquation cracking, which in turn increases backfilling.

Acknowledgments

This work was supported by the National Science Foundation under Grant No. DMR-0098776. The authors thank Bruce Albrecht and Todd Holverson of Miller Electric Manufacturing Company, Appleton, Wis., for donating the welding equipment used in the present study.

References

1. Kou, S. 2003. *Welding Metallurgy*. 2d ed. New York, N.Y.: John Wiley and Sons. 151, 160–3, 303–39.

2. Dudas, J. H., and Collins, F. R. 1966. Preventing weld cracks in high-strength aluminum alloys. *Welding Journal* 45(6): 241-s to 249-s.

3. Metzger, G. E. 1967. Some mechanical properties of welds in 6061 aluminum alloy sheet. *Welding Journal* 46(10): 457-s to 469-s.

4. Steenbergen, J. E., and Thornton, H. R. 1970. Quantitative determination of the conditions for hot cracking during welding for aluminum alloys. *Welding Journal* 49(2): 61-s to 68-s.

5. Gittos, N. F., and Scott, M. H. 1981. Heat-affected zone cracking of Al-Mg-Si alloys. *Welding Journal* 60(6): 95-s to 103-s.

6. Ma, T., and Den Ouden, G. 1999. Liquation cracking susceptibility of Al-Zn-Mg alloys. *International Journal for the Joining of Materials* (Denmark) 11(3): 61–67.

7. Katoh, M., and Kerr, H. W. 1987. Investigation of heat-affected zone cracking of GTA welds of Al-Mg-Si alloys using the Varestraint test. *Welding Journal* 66(12): 360-s to 368-s.

8. Kerr, H. W., and Katoh, M. 1987. Investigation of heat-affected zone cracking of GMA welds of Al-Mg-Si alloys using the Varestraint test. *Welding Journal* 66(9): 251-s to 259-s.

9. Miyazaki, M., Nishio, K., Katoh, M., Mukae, S., and Kerr, H. W. 1990. Quantitative investigation of heat-affected zone cracking in aluminum alloy 6061. *Welding Journal* 69(9): 362-s to 371-s.

10. Gitter, R., Maier, J., Muller, W., and Schwellinger, P. 1992. Formation and effect of grain boundary openings in AlMgSi alloys caused by welding. *Proceedings of 5th International Conference on Aluminum Weldments*, ed. D. Kosteas, R. Ondra, and F. Ostermann, p. 4.1.1. Munchen, Germany: Technische Universita Munchen.

11. Powell, G. L. F., Baughn, K., Ahmed, N., Dalton, J. W., and Robinson, P. 1995. The cracking of 6000 series aluminum alloys during welding. *Proceedings of International Conference on Materials in Welding and Joining*. Victoria, Australia: Institute of Metals and Materials Australasia, Parkville.

12. Ellis, M. B. D., Gittos, M. F., and Hadley, I. 1997. Significance of liquation cracks in thick section Al-Mg-Si alloy plate. *The Welding Institute Journal* 6(2): 213–255.

13. Schillinger, D. E., Betz, I. G., Hussey, F. W., and Markus, H. 1963. Improving weld strength in 2000 series aluminum alloys. *Welding Journal* 42(6): 269-s to 275-s.

14. Young, J. G. 1968. BWRA experience in the welding of aluminum-zinc-magnesium alloys. *Welding Journal* 47(10): 451-s to 461-s.

15. Lippold, J. C., Nippes, E. F., and Savage, W. F. 1977. An investigation of hot cracking in 5083-O aluminum alloy weldments. *Welding Journal* 56(6): 171-s to 178-s.

16. Huang, C., Kou, S., and Purins, J. R. 2001. Liquation, solidification, segregation and hot cracking in the partially melted zone of Al-4.5Cu welds. *Proceedings of Merton C. Flemings Symposium on Solidification Processing*, ed. R. Abbaschian, H. Brody, and A. Mortensen, 229. Warrendale, Pa.: The Mineral, Metals and Materials Society.

17. Huang, C., and Kou, S. 2000. Partially melted zone in aluminum welds — liquation mechanism and directional solidification. *Welding Journal* 79(5): 113-s to 120-s.

18. Huang, C., and Kou, S. 2002. Liquation mechanisms in multicomponent aluminum alloys during welding. *Welding Journal* 81(10): 211-s to 222-s.

19. Huang, C., and Kou, S. 2001. Partially melted zone in aluminum welds — planar and cellular solidification. *Welding Journal* 80(2): 46-s to 53-s.

20. Huang, C., and Kou, S. 2001. Partially melted zone in aluminum welds — solute segregation and mechanical behavior. *Welding Journal* 80(1): 9-s to 17-s.

21. Borland, J. C., and Rogerson, J. H. 1963. Examination of the patch test for assessing hot cracking tendencies of weld metal. *British Welding Journal* 8:494–499.

22. Savage, W. F., and Lundin, C. D. 1965. The Varestraint test. *Welding Journal* 44(10): 433-s to 442-s.

23. Savage, W. F., and Lundin, C. D. 1966. Application of the Varestraint technique to the study of weldability. *Welding Journal* 45(11): 497-s to 503-s.

24. Huang, C., and Kou, S. Liquation cracking in full-penetration aluminum welds. Submitted to *Welding Journal*.

25. The Aluminum Association. 1982. *Aluminum Standards and Data*. 15. Washington, D.C.

26. Fact sheet. 2000. Choosing shielding for GMA welding. *Welding Journal* 79(1): 18.

27. Kotecki, D. J., Cheever, D. L., and Howden, D. G. 1972. Mechanism of ripple formation during weld solidification. *Welding Journal* 51(8): 386-s to 391-s.

28. Renwick, R. J., and Richardson, R. W. 1983. Experimental investigation of GTA weld pool oscillations. *Welding Journal* 62(2): 29-s to 35-s.

29. Xiao, Y. H., and Den Ouden, G. 1990. A study of GTA weld pool oscillation. *Welding Journal* 69(8): 289–s to 293-s.

30. Xiao, Y. H., and Den Ouden, G. 1993. Weld pool oscillation during GTA welding of mild steel. *Welding Journal* 72(8): 428-s to 434-s.

31. Soresen, C. D., and Eagar, T. W. 1990. Measurement of oscillations in partially penetrated weld pools through spectral analysis. *Journal of Dynamic Systems, Measurement and Control* 112:463–468.

32. Sorensen, C. D., and Eagar, T. W. 1990. Modeling of oscillations in partially penetrated weld pools. *Journal of Dynamic Systems, Measurement and Control* 112: 469–474.

33. Borland, J. C. 1979. Fundamentals of solidification cracking in welds. Part 1. *Welding and Metal Fabrication* (January/February): 19–29.

34. Flemings, M. C. 1974. *Solidification Processing*, 34–36, 160–162, 246–252, and app. B. New York, N. Y.: McGraw-Hill.

35. Savage, W. F., and Dickinson, D. W. 1972. Electron microanalysis of backfilled hot cracks in Inconel 600. *Welding Journal* 51(3): 555-s to 561-s.

36. Liao, F-C., and Liu, S. 1992. Effect of deoxidation sequence on carbon manganese steel weld metal microstructures. *Welding Journal* 71(3): 94-s to 103-s.

37. DuPont, N. J. 1999. Microstructural development and solidification cracking susceptibility of a stabilized stainless steel. *Welding Journal* 78(7): 253-s to 263-s.

38. *Binary Alloy Phase Diagrams*, 1986(1):106. Materials Park, Ohio: American Society for Metals International.

39. Philips, H. W. L. 1959. *Annotated Equilibrium Diagrams of Some Aluminum Alloy Systems*, 42. London, U.K.: The Institute of Metals.

40. *Pandat*, computer software developed by CompuTherm LLC, Madison, Wis.

41. Hatch, J. E. 1984. *Aluminum – Properties and Physical Metallurgy*, 209–210. Materials Park, Ohio: American Society for Metals International.